

# Development of High Efficiency Flywheel Energy Storage System for Power Load-Leveling

\*Jun-ichi Itoh, \*Daisuke Sato, \*Tsuyoshi Nagano, \*Kenta Tanaka, \*Noboru Yamada, and \*\*Koji Kato

\*Nagaoka University of Technology

Niigata, Japan

itoh@vos.nagaokaut.ac.jp

\*\*Sanken Electric Co., Ltd.

Saitama, Japan

k.kato@sanken-ele.co.jp

**Abstract** - This paper introduces the performance of a power leveling system with a 3.0-MJ, 3315-r/min flywheel energy storage. In terms of cost reduction, this system uses low cost ball bearings and general purpose induction motor. Therefore, such a system configurations occurs large loss during standby mode. In order to overcome this problem, low loss design algorithm that focuses on the mechanical loss is applied to the design of the flywheel. From the experimental results, it is confirmed that the charge and discharge efficiency of the mechanical part of the proposed flywheel system is 95.2% (charge 97.9%, discharge 97.5%). Moreover, charging and discharging efficiency are measured to evaluate the prototype flywheel system. In addition, a design approach of the outer rotor type motor for improving the efficiency and the energy density is discussed. From the analysis, it is confirmed that the loss of the PMSM at the rated output is reduced by 71.7% as compared with the induction machine. As a result, it is confirmed that the charging efficiency is 93.3% and the discharging efficiency is 93.1% if the outer rotor PMSM drives the flywheel.

## I. INTRODUCTION

Renewable energy systems, especially a wind turbine and a photovoltaic cell, generate a power fluctuation due to the meteorological conditions. Therefore, these systems require energy buffers to suppress the power fluctuations. In addition, an uninterruptible power supply (UPS) is widely used in order to prevent instantaneous power failure in the data center, the factory and so on. The UPS also needs the energy buffers because the UPS has to supply the power to loads until an emergency generator starts.

Table I shows the characteristics of each energy storage devices. The battery can achieve a high energy density at low cost. However, one of the problems in the battery energy storage is a short life time. In particular, the lifetime depends on an ambient and the number of charge and discharge time. In addition, the battery cannot cope with rapid charge and discharge by a large internal resistance of the battery. On the other hand, an electric double layer capacitor (EDLC) has a high charge and discharge efficiency. Moreover, the rapid charge and discharge is possible because the internal resistance is very small. However, similar to the battery, the lifetime is decreased rapidly due to the influence of the ambient temperature [1]. On the other hand, the flywheels has some advantages: (i) environmental friendly, (ii) low maintenance cost, (iii) long lifetime due to no chemical structure, and (iv) the charge and discharge characteristic of high cycle are excellent. For these reason, the flywheel has attracted attention as an energy storage system[2-12].

TABLE I. Characteristics of each storage devices.

	Flywheel	EDLC	Battery
Energy storage	Kinetic energy	Ion transfer	Chemical reaction
Charge & Discharge of short period	Fast	Fast	Slow
Temperature characteristic	Excellent	Limited by temperature	Limited by temperature
Energy density	Good	Good	Excellent

In recent years, an ultra-high speed rotation of the flywheel has been studied [2-4]. The kinetic energy which is stored in the flywheel is proportional to the square of the rotational speed. Therefore, the magnetic bearings have been studied in order to achieve high energy density. However, the magnetic bearing is required an additional control system [5-7]. In addition, flexibility of this system is low because this system is necessary to design in accordance with the capacity of the power source to be compensated. For these reasons, it can lead to high cost and complexity of the control system of the flywheel system. Therefore, it is necessary to achieve the flywheel systems that do not use a magnetic bearing. Hence, multiple parallel operations using small flywheel systems are assumed in this paper. In this structure, compensation performance is changed by the number of the combined flywheel. Then, high flexibility and high scalability of the flywheel system can be achieved. In this study, general-purpose flywheel system for parallel operation is developed. The proposed flywheel system is configured from commercial products such as general-purpose ball bearings, a general-purpose inverters and an inexpensive microcomputer without the specific device.

In this paper, the effectiveness of the proposed flywheel system is introduced. First, the proposed power control method is evaluated by an operation of the power leveling for the power fluctuation of solar power. The conventional control method requires special design of the inverter because the high-speed response performance is required in order to detect the instantaneous power. On the other hand, the proposed method uses only a standard transducer from the market. After that, the steady state loss is analyzed by using the loss measurement result. The loss can be separated into mechanical losses and electrical losses. Therefore, a factor of the loss in the flywheel system is be clarified from the loss analysis. Next, in order to reduce the bearing loss, the

windage loss and the magnetic fluid seal loss toward higher efficiency, the flywheel is improved. In addition, the energy stored efficiency is measured by experiments in order to evaluate the usefulness of the flywheel system as the energy storage. Next, a design approach of the outer rotor type motor for improving the efficiency and the energy density is discussed. The outer rotor type motor can be easily designed with large output torque as compared to the inner rotor type motor. Therefore, the reduction in the axial direction of the motor is achieved. In this case, the losses of an induction motor and a permanent magnet synchronous motor of equal size are compared. Finally, the efficiency of the improved flywheel system is evaluated from loss analysis and loss estimation.

## II. CONSTRUCTION OF FLYWHEEL ENERGY STORAGE SYSTEM

Fig. 1 shows the configuration of a proposed flywheel system that employs the general purpose motor and ball bearings. In this system, it is possible to store the kinetic energy of the 3.0 MJ at 3315 r/min. Such a low rotation speed region can be applied to a typical ball bearing and general purpose motor. In addition, the flywheel vacuum case and the motor are separated by the magnetic fluid seal. As a result, windage loss can be greatly reduced because it is possible to reduce a pressure in the vacuum case by the vacuum pump. Moreover, vacuum in the vacuum case does not affect the heat dissipation of the motor because the motor and the vacuum case are separated. Therefore, the general purpose motor can be applied to drive the flywheel without adding special cooling mechanism.

Fig. 2 shows the block diagram of the flywheel system including the measurement system and auxiliary devices. In the flywheel system, the induction motor is operated as a generator during deceleration; the kinetic energy is converted into the electrical energy. On the other hand, during acceleration, the electrical energy is stored as the kinetic energy, which is working as a motor. Therefore, this system uses a regenerative converter. Furthermore, an over temperature of the bearing and the motor can be prevented by the oil cooler.

Table II shows the specification of the flywheel. It can be seen that the shape of the flywheel is disk-shaped. It is capable of storing sufficient energy for a low rotational speed by the inertia weight is increased. In addition, the windage loss and the bearing losses are reduced by the reduction in rotational speed. The pressure in a vacuum case is reduced by using a vacuum pump prior to operation in order to reduce the windage loss. In addition, the magnetic fluid seal is adopted to maintain the vacuum in the vacuum case.

Table III shows the estimation of the cost of the proposed system. Note that the material of the flywheel is used chromium-molybdenum steel. Here, cost ratio of the material in flywheel is assumed as 1. On the other hand, cost ratio of the magnetic fluid seal and other components becomes 5.0 to be relative to the material cost of the flywheel. The most of this cost is accounted for the magnetic fluid seal. Therefore, it is necessary to consider the structure which can achieve a sufficient vacuum without the magnetic fluid seal. From the

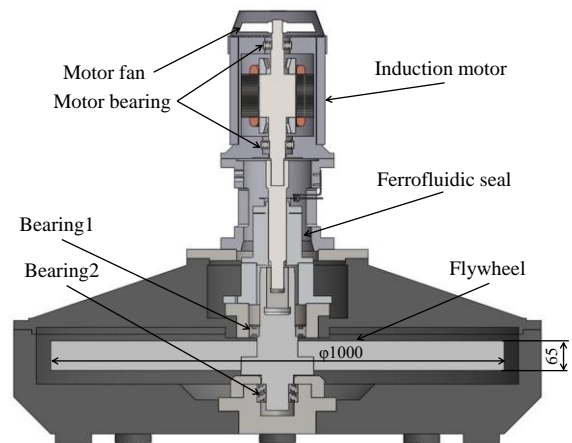


Fig. 1. Configuration of a proposed flywheel system that employs the general purpose motor and ball bearings.

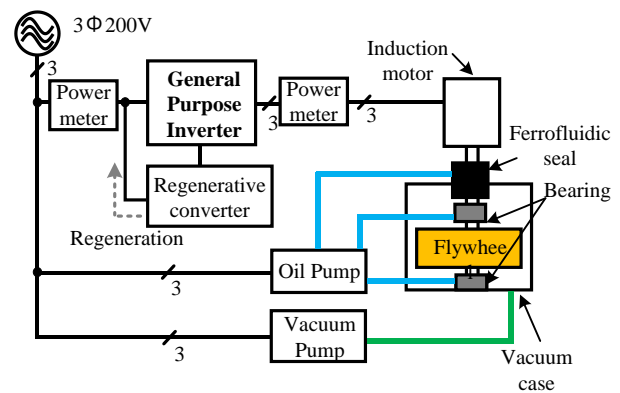


Fig. 2. Block diagram of the flywheel system including the measurement system and the auxiliary devices.

TABLE II. Specifications of the flywheel which is calculated from the low loss design.

Flywheel	Material	SCM440
	Radius	500 mm
	Thickness	65 mm
	Weight of the Flywheel	392 kg
	Stored Energy	3.0 MJ at 3315 r/min
Motor/Generator	MLC1115C (Fuji Electric)	
Inverter	FRN 37G11S-2 (Fuji Electric)	

TABLE III. Estimation of the cost of the proposed system.

Components	Cost ratio
Material cost of Flywheel (SCM440)	1.0
Other material cost	5.5
Power converter	2.9
Induction machine	1.3
Ball bearings	2.6
Other components	5.0
Total cost	18.2

results, it is confirmed that the material cost of the flywheel in the proposed system is very cheap. However, the total cost of the entire system including the processing cost and the other components becomes very expensive. Therefore, it is possible to achieve a more reasonable system by improving the manufacturing method and structure.

Next, the cost of the proposed system is compared with other energy storage devices. The comparison condition is the same as the energy storage. From the reference [12], total cost of EDLC energy storage systems becomes approximately 25% higher as compared to the proposed flywheel system. Note that specification of the capacitor to be used is as follows: the rated voltage is 2.5 V, a capacitance is 2700 F, and the cost per unit is \$30. From these results, it is confirmed that the proposed system can achieve a lower cost than an EDLC energy storage system depending on the manufacturing cost. However, the reduction of processing cost and component cost are important issue for practical application of the flywheel.

### III. VERIFICATION OF POWER LEVELING CONTROL

In the flywheel system, when induction machine is operated as a generator during deceleration, kinetic energy is converted into the electrical energy. On the other hand, during acceleration, the electrical energy is stored as kinetic energy, which is working as a motor. In general, inexpensive general purpose inverter can only provide speed command. Therefore, the charging and discharging power is controlled by the speed of the flywheel.

The kinetic energy of a body of revolution is expressed by (1).

$$E = \frac{1}{2} J \omega^2 \dots\dots\dots (1)$$

where,  $J$  is the moment of inertia [kgm<sup>2</sup>] and  $\omega$  is the angular velocity of the body revolution [rad/s]. In addition, the speed command  $\omega^*$  which shown in Fig. 2 can be obtained by transforming (1). On the other hand, the output power of the flywheel can be obtained by differentiating the both sides of (1) from the relation between the rotational kinetic energy and power. Thus, the output power is expressed by (2).

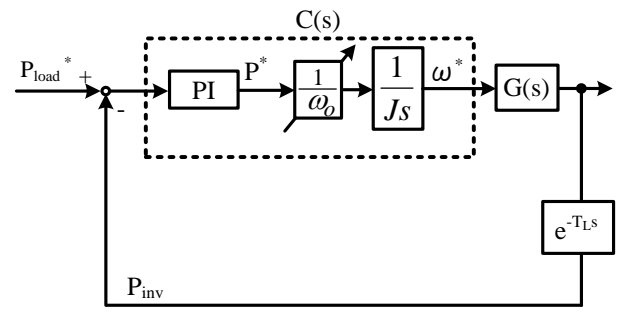
$$P = J\omega \frac{d\omega}{dt} \dots\dots\dots (2)$$

Accordingly, the regenerative power of the flywheel is proportional to the product of the rotational angular velocity and angular acceleration. The speed command value for the regenerative power of the flywheel is given by (3).

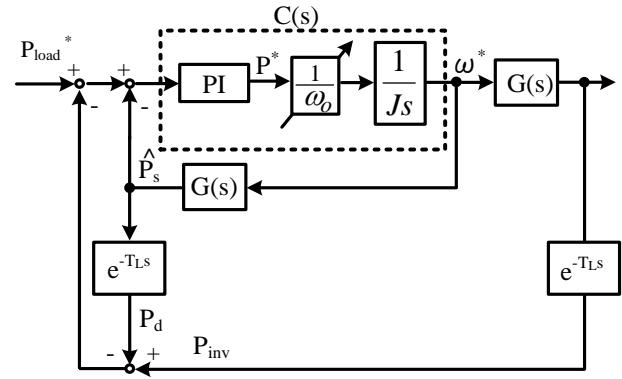
$$\omega^* = \frac{1}{J} \int \frac{P^*}{\omega_o} dt \dots\dots\dots (3)$$

where,  $\omega_o$  is the rotational angular velocity of the previous sampling time and  $P^*$  is the output of the PI controller.

Furthermore, the discrete system of equation (3) is given by (4).



(a) Without smith predictor.



(b) With smith predictor.

Fig. 3. Block diagram of time delay compensation scheme based on Smith predictor. This compensation eliminates the effect of time delay by estimating the output of the controlled object  $G(s)$  after the lapse of time delay.

$$\omega_n = \omega_{n-1} + \frac{1}{J} \frac{P^*}{\omega_{n-1}} \Delta t \dots\dots\dots (4)$$

where,  $\omega_{n-1}$  is the speed command value of the previous sampling time and  $\Delta t$  is the sampling time of the controller.

In this system, the regenerative power is obtained from an inexpensive power meter that the sampling time is 400 msec. In such a system, the control may become unstable by setting a high proportional gain to improve the response. In this paper, the control performance is improved by the Smith delay time compensation scheme.

Fig. 3(a) shows the block diagram of the typical feedback control system. Note that the change of the rotational angular velocity is sufficiently slower than the processing time of the control system. Therefore, the rotational angular velocity of the previous sampling time is treated as a constant value  $\omega_o$ . The characteristic equation of this control system is given by (5).

$$1 + C(s)G(s)e^{-T_Ls} = 0 \dots\dots\dots (5)$$

Fig. 3(b) shows the block diagram with the Smith predictor to power control. This compensation eliminates the effect of delay time by estimating the output of the controlled object  $G(s)$  after the lapse of delay time. The characteristic equation

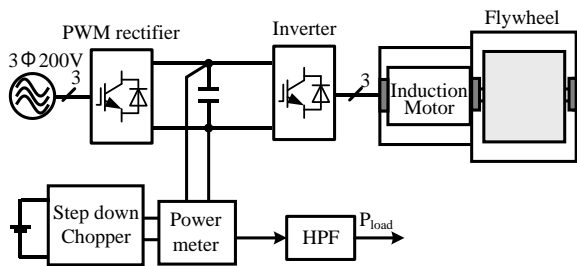


Fig.4. Configuration of the experimental system for the power fluctuation compensation.

is given by (6).

$$1 + C(s)G(s) = 0 \dots\dots\dots(6)$$

Therefore, the control performance can be improved from this equation. In other words, the delay time element has been removed from the characteristic equation.

Fig. 4 shows the power leveling control system. Note that the rotation speed is 5500 r/min at steady state. In the experiment, the power fluctuation is reproduced by a step-down chopper. In addition, the flywheel power command value is extracted from a high pass filter (HPF) that cutoff frequency is set to 0.0025 Hz. The prototype system is intended to compensate for a short cycle of the power fluctuation. Therefore, the cutoff frequency of the HPF is set to low frequency.

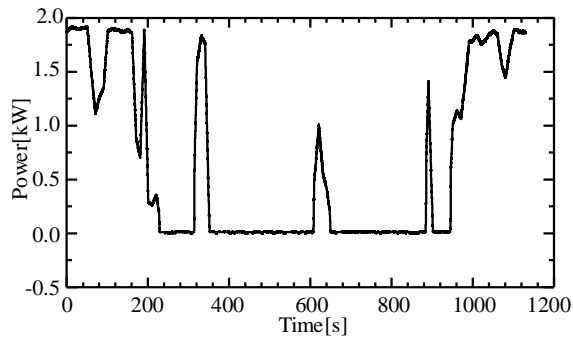
Fig. 5(a) shows the power fluctuation pattern which uses a part of generation power by PV panels. From this figure, the generation power of the solar cell has a rapid power fluctuation of approximately 2 kW.

Fig. 5(b) shows the output power of the flywheel and Fig. 5(c) shows the grid power. From these results, the fluctuation of generated power is compensated by the output power of the flywheel. Therefore, the sudden fluctuation due to power fluctuation does not occur on the grid power.

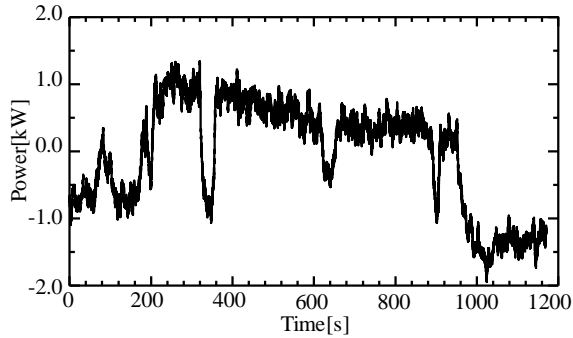
Fig. 5(d) shows the rotation speed of the flywheel. As a result, it is confirmed that the sudden speed variation does not occurs. According to the Fig. 5(c), the high frequency ripple occurs in the grid power. This ripple is caused by the influence of the power detection delay time. This problem can be improved by the optimization of the control gain.

Fig. 6 shows the harmonic analysis of the fluctuation pattern and the grid power. The experimental conditions are similar to Fig. 5. As the result, it is confirmed that the fluctuation pattern has large frequency component between 0.01 Hz and 0.004 Hz. By contrast, the grid power fluctuations over 0.004 Hz is reduced 84.6 % by the power leveling control.

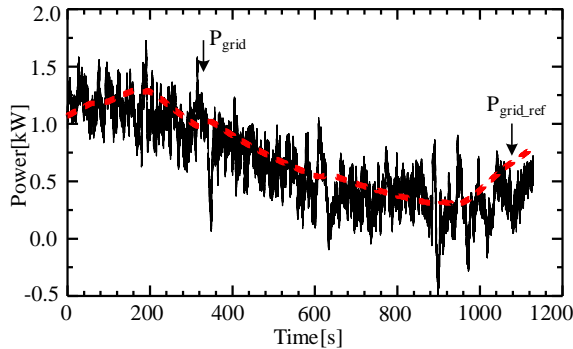
Fig. 7 shows the measurement result of the steady state loss in experiment with prototype FESS as shown in Fig. 1. In this experiment, the rotation speed is 3315 r/min, the vacuum case is kept at 500 Pa. The mechanical loss and the electrical loss are separated by a free-run test at the beginning. Free-run test is a test for electrically disconnecting the inverter and the motor with the energy stored in the flywheel. In this state, the stored energy is



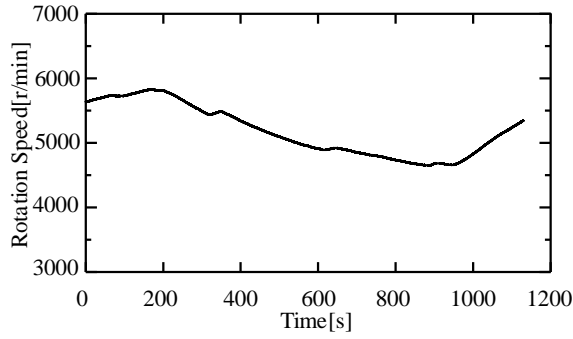
(a) Fluctuation pattern



(b) Output power of the Flywheel



(c) Grid power



(d) Rotation speed

Fig. 5. Experimental results of the power fluctuation compensation control when applying Smith predictor (Rotation speed is 5500r/min).

consumed only by mechanical loss. Therefore, the mechanical loss is calculated from the time until the stored energy is consumed. From the results, it is confirmed that the bearing loss accounts for 48.6% of all mechanical loss.

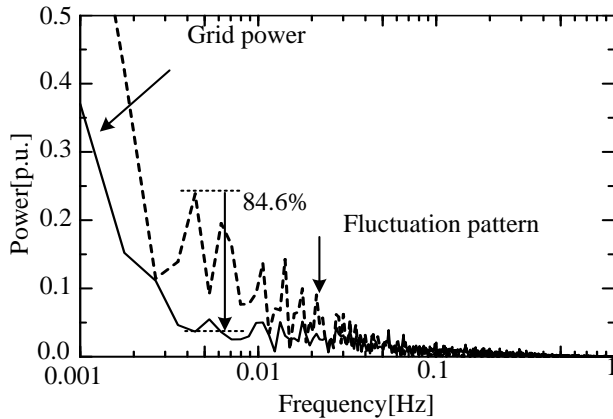


Fig.6. Harmonic analysis during the power fluctuation compensation. The experimental conditions are similar to Fig. 5.

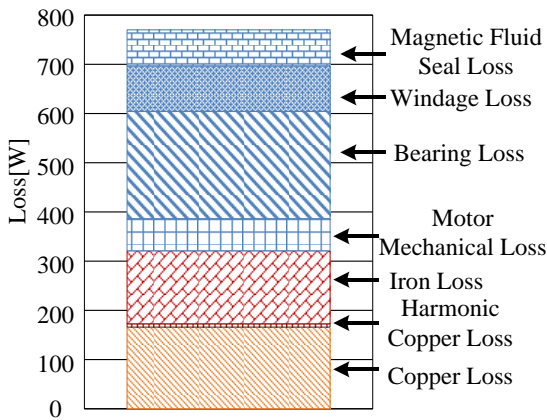


Fig. 7. Loss analysis results at the rated energy storage. In the experiment, the steady rotation speed is 3315 r/min and the pressure of the vacuum case is 500 Pa.

Additionally, the electrical losses of the motor are accounted for 41.7% of the total loss. Therefore, it is necessary to improve the motor efficiency and reducing the bearing loss toward higher efficiency.

#### IV. IMPROVEMENT OF THE FLYWHEEL SYSTEM

##### A. Improvement toward higher efficiency

The previous chapter clarifies that the bearing loss, the sum of the windage loss and the magnetic fluid seal loss account for 57% of the total loss of the proposed flywheel system. In order to reduce the bearing loss, the windage loss and the magnetic fluid seal loss toward higher efficiency, the flywheel is improved.

Fig. 8 shows the configuration of a proposed flywheel system after the system of Fig. 1 is improved in order to reduce the bearing loss, the windage loss and the magnetic fluid seal loss. Table IV shows the specification of the improved flywheel system. In this system, it is possible to store the kinetic energy of the 3.0 MJ at 2900 r/min because the shape of the flywheel is changed in order to achieve the moment of inertia with lighter weight of the flywheel. In addition, the flywheel vacuum case and the motor are separated by not the magnetic fluid seal but the magnetic coupling. The higher pressure in the vacuum case can be

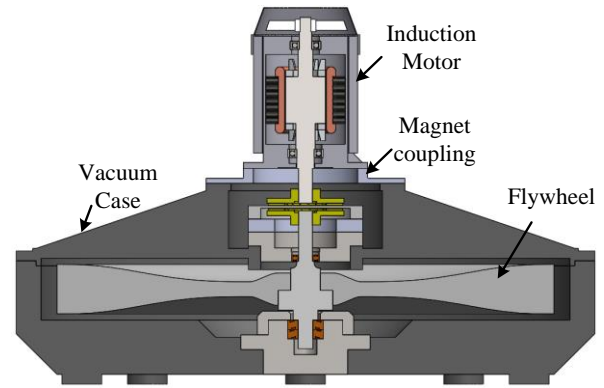


Fig. 8. Configuration of a proposed flywheel system that comprises a general purpose motor and ball bearings after the system of Fig. 1 is improved.

Table IV. Specifications of the flywheel which is calculated from the low loss design.

Flywheel	Material	SCM440
	Radius	500 mm
	Thickness	65 mm
	Weight of the Flywheel	392 kg
	Stored Energy	3.0 MJ at 2900 r/min
Motor/Generator	MLC1115C (Fuji Electric)	
Inverter	FRN 37G11S-2 (Fuji Electric)	

kept by using the magnetic coupling than the magnetic fluid seal because the magnetic coupling is used. As a result, windage loss can be reduced as compared with the magnetic fluid seal because the magnetic coupling connects magnetically the flywheel vacuum case with the motor. Moreover, the diameter of the ball bearing is changed in order to reduce the bearing loss.

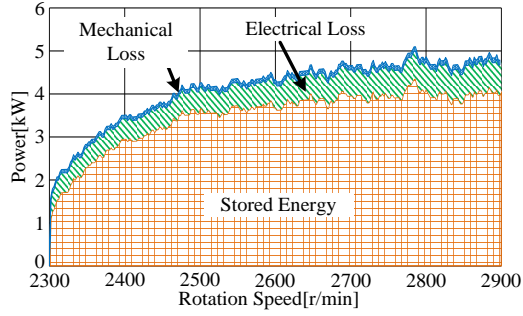
##### B. Analysis of the energy storage efficiency

In this section, the energy storage efficiency of the improved prototype system (Fig. 8) is analyzed. This property is divided into a discharging efficiency and a charging efficiency. The charging efficiency is the ratio of the energy consumed for storing the desired energy. On the other hand, the discharging efficiency is the ratio of actual energy can be released with respect to stored energy.

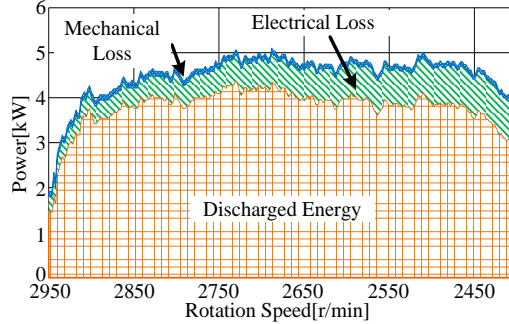
Fig. 9 shows the experimental results of (a) the energy storage and (b) the energy discharge. In the experiment of energy storage, the flywheel is accelerated from 2300 r/min to 2900 r/min. In the discharge test, the flywheel is decelerated from 2900 r/min to 2300 r/min. The stored energy is calculated using (6) from the rotational angular velocity and the moment of inertia of the flywheel  $J$ .

$$E = \frac{1}{2} J \omega^2 \dots\dots\dots (6)$$

From this equation, it is calculated that the amount of the energy change is 1 MJ when the rotational speed changes from 2300 r/min to 2900 r/min. Next, the energy storage efficiency is calculated using the experimental results. Note



(a) Charging efficiency



(b) Discharging efficiency

Fig. 9. Measurement results of the charging and discharging efficiency.

that, the charging efficiency is the ratio of the input energy to the stored energy. On the other hand, the discharging efficiency is the ratio of the decreasing of the kinetic energy to regenerative energy. If only the mechanical loss is considered, it is confirmed that the achieved charging efficiency is 97.9 % and the achieved discharging efficiency is 97.5 %. Therefore, the total achieved efficiency is 95.2 %. On the other hand, if the motor loss is considered, the achieved charging efficiency is 80.7 % and the achieved discharging efficiency is 75.1 %. Therefore, the total achieved efficiency is 60.7 %. This cause of low efficiency is mainly the additional loss caused by introducing the induction motor driving the flywheel. Thus, it is necessary to apply the PMSM to achieve high efficiency of the entire flywheel system.

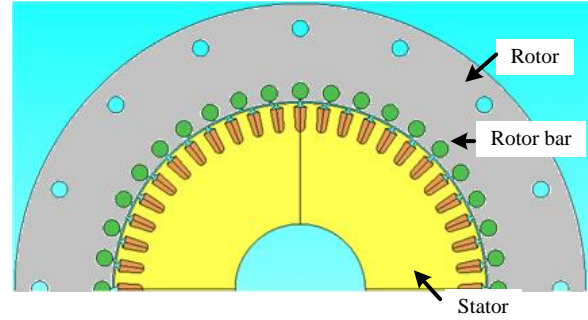
The discharging efficiency of the energy storage devices is as follows: the lead acid battery is 75-85%, a redox flow battery is approximately 70%, an EDLC is approximately 90%. Therefore, it is confirmed that the energy storage efficiency of the prototype flywheel is about the same as the current main power storage device.

## V. IMPROVEMENT OF MOTOR EFFICIENCY

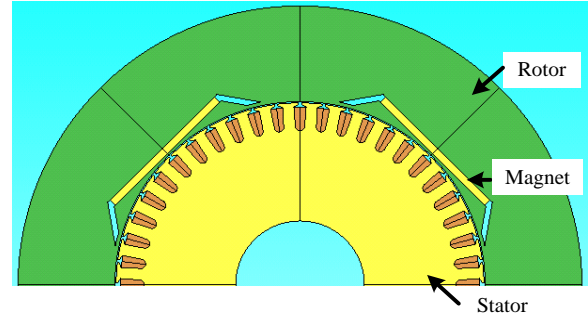
Table V shows comparison of the characteristics between inner rotor type motor and outer rotor type motor. In order to improve the efficiency and the energy density of the proposed flywheel system, a design approach of the outer rotor type motor is discussed in this chapter. The general purpose induction motor can be used when the motor is located outside of the vacuum case. However, due to the limitation of the magnet size, the inner rotor type motor is relatively large in the rotation axis direction. Thus, the energy density of the flywheel system becomes lower. In contrast, the outer rotor

Table V. Comparison of the characteristics between inner rotor type motor and outer rotor type motor.

Evaluation criteria	Inner rotor type	Outer rotor type
Limitation of magnet size	Limited	No Limited
Winding coils	Difficult	Easy
Heat dissipation	Easy	Difficult
Inertia moment of motor	Small	Large



(a) Induction motor model



(b) Permanent magnet synchronous motor model

Fig.10. Analysis model.

type motor can be easily designed with large output torque as compared to the inner rotor type because the magnet size is not limited. Therefore, the reduction in the axial direction of the motor is achieved. For these reasons, an outer rotor type motor can be applied in order to improve the energy density and efficiency of the flywheel system.

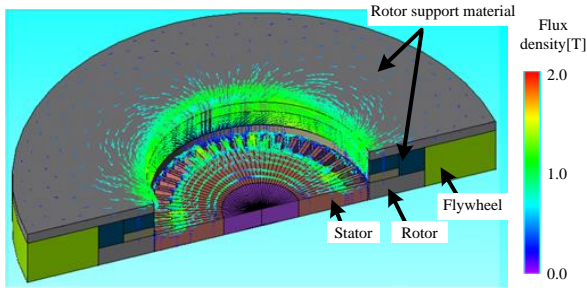
Fig. 10 shows the induction machine model and PMSM model. In this flywheel system, it is possible to store the kinetic energy of the 3.0 MJ at 6000 r/min. Moreover, the shape of the stator core is the same in the PMSM and the induction machine type. Table VI show the specification of the proposed system.

Fig. 11 shows the three-dimensional analysis of (a) the induction machine and (b) PMSM. In the three-dimensional analysis, the magnetic flux flowing in the axial direction and the inertial body are analyzed. An analysis condition is a sine wave source both in the analysis of the PMSM and the induction machine. In addition, the magnetic material SS400 is applied to the flywheel and the rotor support. From the

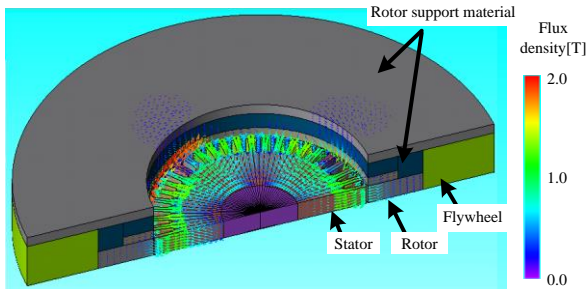
TABLE VI. Estimation of the cost of the proposed system.

(a) Induction motor	
Outer diameter of rotor	460 mm
Outer diameter of stator	300 mm
Air gap length	1 mm
Number of slots	48
Number of rotor bars	40
Pole number	4
Number of coil turns	12
Iron	35JN230
Rotor bar	Copper

(b) Permanent magnet synchronous motor	
Outer diameter of rotor	460 mm
Outer diameter of stator	300 mm
Air gap length	1.5 mm
Number of slots	48
Pole number	4
Number of coil turns	3
Iron	35JN230
Magnet	NMX-S45SH



(a) Induction motor model



(b) Permanent magnet synchronous motor model

Fig.11. Analysis result

analysis, it is confirmed that the magnetic flux leaking from the rotor flows in the support material and the flywheel. Therefore, the analysis of the proposed FESS is necessary to consider the flywheel and the rotor support.

Fig. 12 shows the comparison of loss with respect to the load conditions. Note that, the loss is normalized by the output power. From the analysis, it is confirmed that the electrical loss of the PMSM at the rated output is reduced by 71.7% as compared with the induction machine. In particular, the effect of reducing the copper loss is significant. The cause of the loss reduction is that the secondary copper loss does not occur in the PMSM. This is because the secondary magnetic flux is generated by the rotor magnets in the PMSM. Similarly, it is confirmed that the PMSM can achieve a low loss as compared with the induction machine in the

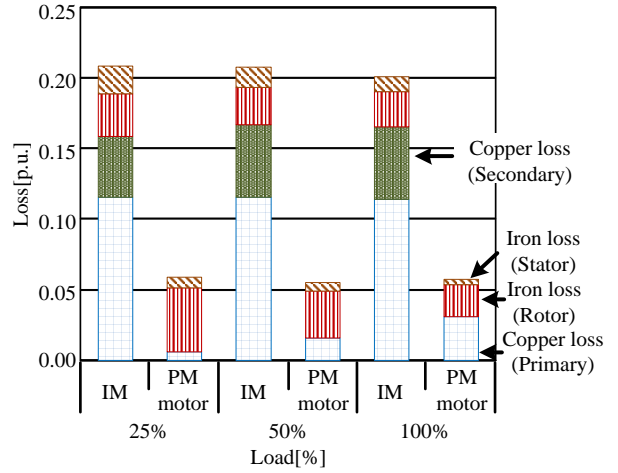


Fig. 12. Comparison of loss with respect to the load conditions

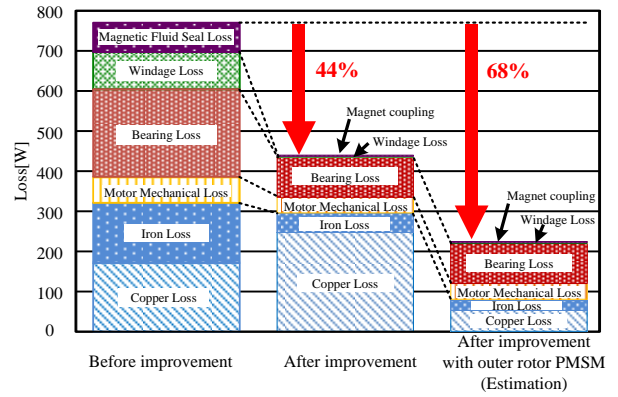


Fig. 13. Loss analysis results at the rated energy storage. In the experiment, the steady rotation speed is 2900 r/min and the pressure of the vacuum case is 20 Pa.

entire load range. From the analysis, the effectiveness of the PMSM type flywheel is verified by the simulation.

Fig. 13 shows the analysis result of the steady state loss in the experiment with prototype flywheel system before and after the improvement. In the experiment of the flywheel system after the improvement, the rotational speed is 2900 r/min and the pressure in the vacuum case is kept at 20 Pa. The mechanical loss and electrical loss are separated respectively by a free-run test as well as Fig. 7. From the analysis results using the induction machine, the motor loss contributes 68.1% of the total loss. On the other hand, the total loss after the improvement is 44% lower than before the improvement because the mechanical loss is reduced by the improvement. As a result, it is confirmed that flywheel after the improvement achieves low loss as compared with the flywheel before the improvement. In addition, the loss when the motor is changed to the outer rotor PMSM is estimated. From the results, the total loss is reduced by 68% to the loss before the improvement. Moreover, the discharging efficiency be achieved to 93.3% and the charging efficiency be achieved to 93.1% if the motor is changed to the outer rotor PMSM.

## VI. CONCLUSION

This paper introduces the performance of a power leveling system with a 3.0-MJ, 3315-r/min flywheel energy storage. In this proposed system, simplification of the system is achieved by applying the general purpose induction machine and the ball bearings. From the loss analysis, it is confirmed that the bearing loss accounts for 48.6% of all mechanical loss. In addition, in order to reduce the bearing loss, the windage loss and the magnetic fluid seal loss, the proposed flywheel system is improved. Moreover, the energy storage efficiency is measured by experiments. Towards higher efficiency, authors will consider the design approach of the outer rotor type motor. From the analysis, it is confirmed that the loss of the PMSM at the rated output is reduced by 71.7% as compared with the induction machine. Similarly, it is confirmed that the PMSM can achieve a low loss as compared with the induction machine in the entire load range. From the analysis, the effectiveness of flywheel system with the outer rotor type PMSM is verified by the simulation. As a result, it is confirmed that the charging efficiency is 93.3% and the discharging efficiency is 93.1% if the outer rotor PMSM drives the flywheel. Therefore, it is confirmed that the energy storage efficiency of the prototype flywheel is about the same as the current main power storage device.

## REFERENCES

- [1] M.Uno, K.Tanaka," Accelerated Charge-Discharge Cycling Test and Cycle Life Prediction Model for Supercapacitors in Alternative Battery Applications" IEEE Trans on industrial electronics, Vol.60, No.6, pp.2131-2138(2013)
- [2] C. Zhang, K.J. Tseng, T.D. Nguyen, S. Zhang:"Design and loss analysis of a high speed flywheel energy storage system based on axial-flux flywheel-rotor electric machines", IPEC-Sapporo, pp.886-891(2010)
- [3] Frank N. Werfel, Uta Floegel-Delor, Thomas Riedel, Rolf Rothfeld, Dieter Wippich, Bernd Goebel, Gerhard Reiner, and Niels Wehlau:"A Compact HTS 5 kWh/250 kW Flywheel Energy Storage System",IEEE Transactions on Applied Superconductivity,Vol.17,No.2, pp.2138-2141(2007)
- [4] M. Strasik, P. E. Johnson, A. C. Day, J. Mittleider, M. D. Higgins, J. Edwards, J. R. Schindler, K. E. McCrary, C. R. McIver, D. Carlson, J. F. Gonder, and J. R. Hull:" Design, Fabrication, and Test of a 5-kWh/100-kW Flywheel Energy Storage Utilizing a High-Temperature Superconducting Bearing", IEEE Transactions on Applied Superconductivity., Vol. 17, No.2, pp.2133-2137(2007)
- [5] B.H.Kenny, P.E.Kascak, R.Jansen, T.Dever, W.Santiago,"Control of a High-speed Flywheel System for Energy storage in Space Applications",IEEE Trans on industry applications, Vol. 41, No. 4, pp. 1029-1038(2005)
- [6] Z.Kohari, Z.Nadudvari, L.Szlama, M.Keresztesi, I.Csaki,"Test Results of a Compact Disk-type Motor/Generator Unit with Superconducting Bearings for Flywheel Energy Storage Systems with Ultra-low Idling Losses",IEEE Trans on applied superconductivity, Vol. 21, No. 3, pp. 1497-1501(2011)
- [7] K.Murakami, M.Komori, H.Mitsuda,"Flywheel Energy Storage System Using SMB and PMB",IEEE Trans on applied superconductivity, Vol. 17, No. 2, pp. 2146-2149(2007)
- [8] K. Tanaka, Y. Ohnuma, T. Fujimori, J. Itoh, N. Yamada: "Loss Analysis of a Flywheel Energy Storage System for an Energy Cache Operation", SPC Ishikawa, SPC-11-006, MD-11-032(2011)
- [9] K. Tanaka, J. Itoh, S. Matsuo, N. Yamada: "Regenerative Power Control Method of Flywheel Power Leveling System Using Smith Dead Time Compensation Method", IEEJ JIASC, No. 1-58(2012)
- [10] N. Yamada, T. Fujimori, S. Wakashima,"Prediction of Mechanical Losses of Small-scale Flywheel Energy Storage System", Transactions of the Japan Society of Mechanical Engineers, Series B, Vol.78, No.789(2012)
- [11] T. Ogura, J. Itoh: "Evaluation of Total Loss of Both an Inverter and Motor Depending on Modulation Strategies", SPC Hamamatsu, Spc-09-184, LD-09-074(2009)
- [12] M. Ortuzar, J. Moreno, J. Dixon, "Ultracapacitor-based Auxiliary Energy System for an Electric Vehicle: Implementation and Evaluation", IEEE Trans on industrial electronics, Vol. 54, No. 4, pp.2147-2156(2007)